Article

A Novel Closed-Loop Control to Solve Light Source Power Fluctuations in the Fiber-Optic Gyroscope

Shijie Zheng, Mengyu Ren, Xin Luo, Hangyu Zhang and Guoying Feng *

Institute of Laser & Micro/Nano Engineering, College of Electronics & Information Engineering,
Sichuan University, Chengdu 610065, China
* Correspondence: guoing_feng@scu.edu.cn; Tel.: +86-133-080-18393

Abstract: The performance of a gyroscope is directly affected by the fluctuations in the light source power (LSP) in an interferometric fiber-optic gyroscope (IFOG). Therefore, it is important to compensate for fluctuations in the LSP. When the feedback phase generated by the step wave completely cancels the Sagnac phase in real-time, the error signal of the gyroscope is linearly related to the differential signal of the LSP, otherwise, the error signal of the gyroscope is uncertain. Herein, we present two compensation methods to compensate for the error of the gyroscope when the error is uncertain, which are double period modulation (DPM) and triple period modulation (TPM). Compared with the TPM, DPM has better performance, but it increases the requirements for the circuit. TPM has lower requirements for the circuit and is more suitable for small fiber-coil applications. The experimental results show that, when the frequency of the LSP fluctuation is relatively low (1 kHz and 2 kHz), DPM and TPM do not differ significantly in terms of performance; both of them can achieve an improvement of about 95% in bias stability. When the frequency of the LSP fluctuation is relatively high (4 kHz, 8 kHz and 16 kHz), DPM and TPM can achieve about 95% and 88% improvement in bias stability, respectively.

Keywords: power fluctuation; crosstalk; compensation; modulation and demodulation

1. Introduction

After decades of development, the technology of IFOG has become very mature, and it is widely used in aviation, navigation, satellite navigation, and other fields [1,2]. In recent years, miniaturization and lowering costs have become hot topics of IFOG [3–7]. With the development of integrated chip technology, optical components of IFOG have gradually begun to be integrated into the chip, making miniaturization and low cost for IFOG possible. In 2011, GENER8 Co. and the Centre for Photonics (Ipswich, UK) integrated 24 optical components into a single chip [8]. In 2014, Bookham Co. integrated the light source, coupler, phase modulator and photodiode into a single chip, and its IFOG was successfully verified on a missile INS [9]. In 2017, a light source, three photodetectors, two phase modulators, and two couplers were integrated into a single chip by Tran et al. [10]. In 2019, KVH Co. integrated a polarizer and two Y waveguides into a single chip, its IFOGs achieving a bias stability of 0.048 °/h [11]. In 2022, Shang et al. produced an IFOG with a size of only 3 cm × 3 cm × 3 cm [12].

A superluminescent diode (SLD) is generally used in a low-cost IFOG, and the light source is generally packaged with an SLD, a thermoelectric cooler (TEC) and a thermistor. The package size is very large, and the driving circuit of the light source is also complicated. This is one of the reasons why there are almost no successful cases of miniaturized light sources for an IFOG, although Shang et al. realized the integration of a light source, photodetector and coupler in 2020. With the limitation of the volume of the TEC, the size after packaging still exceeded 26 mm [3]. In addition, a light source, three photodetectors, two phase modulators, and two couplers were integrated into single chip by Tran et al. in

2017, but the performance of these fiber-optic gyroscopes is relatively low, at just about 0.53 °/h [10]. Simplifying the light source of IFOG is an unavoidable step in the process of miniaturization and cost reduction, but simplifying the light source inevitably compromises its stability, which has a significant impact on the performance of the gyroscope [13–15].

There are two closed-loop control processes in a traditional IFOG, which are phase closed-loop control and 2π voltage closed-loop control [16,17]. Phase closed-loop control solves the problem of IFOG sensitivity reduction at high rotation rates, and 2π voltage closed-loop control solves the problem of the scale factor drift of the phase modulator. In this paper, we propose another closed-loop control to solve the problem of the fluctuation of LSP reducing the performance of the IFOG. Using our method, the compensation of the LSP fluctuation is realized without increasing the hardware cost. In the experiment, we modulate a variety of different waveforms, amplitudes, and frequencies for driving the current of the light source, and the experimental results prove that our method can reduce the impact of LSP fluctuations by about 95%.

2. Analysis and Simulation

2.1. Error Analysis

The IFOG system consists of a light source, coupler, phase modulator, fiber coil, photodetector and logic processor, as shown in Figure 1c.
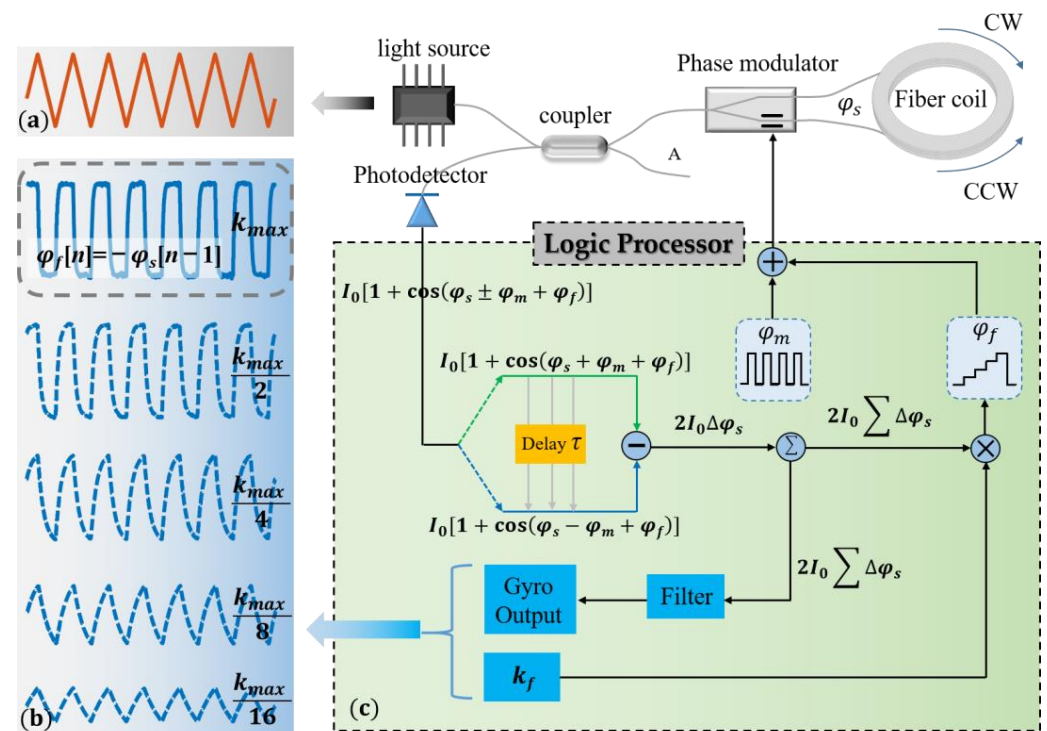
Figure 1. The system composition of IFOG, the signal of LSP and the signal of the output of IFOG. (**a**) Light source power signal. (**b**) The output signal of IFOG. (**c**) System components of an IFOG.

There is a Sagnac phase φ_s between the two beams of light rotating in opposite directions in the fiber coil, when the fiber coil is rotating. The Sagnac phase φ_s is proportional to the rotation speed, resulting in a change in the intensity of the interferometric light. [18]. The Sagnac phase φ_s can be expressed as:

$$\varphi_s = \frac{2\pi L D \Omega_{\text{in}}}{\lambda c} \tag{1}$$

where L is the length of the fiber coil, D is the diameter of the fiber coil, Ω_{in} is the rotation speed, λ is the average wavelength of light, and c is the speed of light in a vacuum. After

closed-loop control of the gyroscope, if the total gain of the detection circuit is G, the output signal of IFOG can be expressed as:

$$\Omega[n] = 2GI_0 \sum_{i=1}^{n} \Delta\varphi_s[i] \tag{2}$$

where n is a discrete signal sequence with a period of 2τ, $\Delta\varphi_s$ is the increment of φ_s, and I_0 is proportional to LSP. Usually, we think that I_0 is a constant. However, the LSP certainly fluctuates when the working environment of the gyroscope changes [19–21]. In addition, in the process of miniaturization and cost reduction, the light source and its drive circuit might be simplified, compromising the stability of the light source. Therefore, it is crucial to study the influence of LSP fluctuation on the gyroscope, and to compensate for them.

Due to LSP fluctuations, there will be a difference in the average light intensity between the first half period and the second half period, and this difference will be mistakenly thought by the IFOG system to be caused by the change in rotation speed. In the phase closed-loop control, the feedback phase φ_f generated by the step wave will follow the rotation speed signal in real-time. After the closed-loop control phase, this difference in light intensity will eventually lead to an error in the output of the gyroscope.

The feedback phase φ_f is linearly related to the height of the step wave. By integrating the light intensity difference between the first half period and the second half period, and then multiplying by a coefficient k_f, we obtain a value that determines the height of the step wave, as shown in Figure 1c. The larger the coefficient of k_f, the faster the response of the gyroscope. However, there is a maximum value k_{max} which is a constant determined by the system, and when k_f exceeds k_{max}, the system is unstable.

When $k_f \rightarrow k_{max}$, the feedback phase φ_f generated by the step wave can almost completely cancel the light intensity difference of the previous period and, as a result, condition ($\varphi_f[n] = -\varphi_s[n-1]$) is satisfied. According to our previous research work [22], if the differential signal of the light intensity, $I_0(t)$, is $\beta(t)$, the output of the gyroscope can be expressed as follows [22]:

$$\begin{aligned}\Omega[n] &= 2G\sum_{i=1}^{n} I_0[n]\Delta\varphi_s[i] \\ &+ G\tau(\beta[n] - \beta[0])\end{aligned} \tag{3}$$

where τ is the time required for light to pass through the fiber coil, and $I_0[n]$ is the average of light intensity, $I_0(t)$, in one period of the gyroscope. $\beta[n]$ is the discrete signal of the differential signal of the LSP, which can be expressed as follows:

$$\beta[n] = \frac{1}{2\tau}\int_{2n\tau-2\tau}^{2n\tau} \beta(t)dt \tag{4}$$

After considering the fluctuations in the LSP, the output signal of the gyroscope not only contains the desired Sagnac phase information, but also contains the undesired differential signal of the LSP. Subtracting a certain proportion of the LSP differential signal from the output signal of the gyroscope can effectively reduce the error caused by the fluctuation in LSP. However, this compensation method can only be used when condition ($k_f \rightarrow k_{max}$) is satisfied.

The smaller the value of coefficient k_f, the lower the system noise, and the higher the value of coefficient k_f, the better the dynamic performance of the IFOG. That is to say, in practical applications, the coefficient k_f is uncertain, and the prerequisite, ($k_f \rightarrow k_{max}$), of the compensation method used in the previous research may not be satisfied [22].

When $0 < k_f < k_{max}$, the crosstalk signal in the output signal of the gyroscope will no longer be the differential signal of the light source power. We consider an extreme case, when $k_f \rightarrow 0$, φ_f hardly changes in a short time, and the output of the gyroscope can be expressed as:

$$\begin{aligned}\Omega[n] &= G\sum_{i=1}^{n}\left(I_B[n] - I_A[n]\right) \\ &= \frac{1}{2}G\sum_{i=1}^{n}\int_{2n\tau-2\tau}^{2n\tau}\beta(t)dt \\ &= \frac{1}{2}G[I(2n\tau) - I(0)]\end{aligned} \tag{5}$$

where $I_A[n]$ and $I_B[n]$ can be expressed as follows.

$$I_A[n] = I_0(2n\tau - 2\tau) + \frac{1}{2}\int_{2n\tau-2\tau}^{2n\tau-\tau}\beta(t)dt \tag{6}$$

$$I_B[n] = I_0(2n\tau - 2\tau) + \int_{2n\tau-2\tau}^{2n\tau-\tau}\beta(t)dt + \frac{1}{2}\int_{2n\tau-\tau}^{2n\tau}\beta(t)dt \tag{7}$$

When $k_f \to k_{max}$, Equation (3) indicates that the crosstalk in the output of the gyroscope is LSP's differential signal. However, Equation (5) shows that the crosstalk in the output of the gyroscope is the LSP signal rather than the LSP's differential signal under the condition that $k_f \to 0$. That is to say, in the process of k_f gradually decreasing from k_{max}, the crosstalk in the output of the gyroscope will gradually change from the LSP's differential signal to the LSP signal. For example, when the LSP is a triangle wave, in the process of k_f gradually decreasing from k_{max}, the crosstalk in the output of the gyroscope will gradually change from a square signal to a triangle signal, as shown in Figure 1a,b. Therefore, the impact of LSP fluctuations varies with coefficient k_f. We have given the solution to the case of ($k_f \to k_{max}$), in our previous research work [22]. In this paper, we present a compensation scheme for any k_f, a significant advance on previous work.

2.2. Error Simulation

We simulated the output signal of the IFOG with different LSPs and different coefficients of k_f. When $k_f \to k_{max}$, the LSP is set to a square wave, triangle wave, and sine wave, and the amplitude is 1% of the total power. The result is shown in Figure 2a.
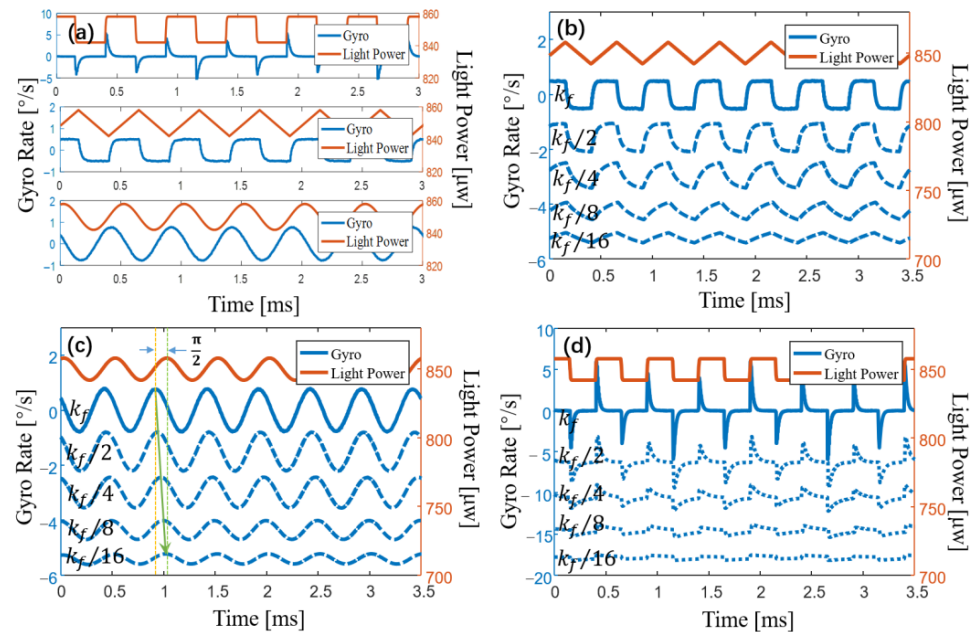
Figure 2. Simulation of crosstalk signal of the IFOG with different coefficients and waveforms. (**a**) When $k_f \to k_{max}$, the output signal of the gyroscope is shown when the light source power is set to a square wave, triangle wave and sine wave, respectively. (**b**–**d**) As k_f gradually decreases, the output signal of the gyroscope is shown when the light source power is set to a square wave, triangle wave, and sine wave, respectively.

When $k_f \to k_{max}$, the simulation results are shown in Figure 2a, which are basically consistent with Equation (3). That is, the differential signal of the LSP is crosstalked into the output of the gyroscope. Spike pulses appear when the square wave jumps, which is in line with the results of our analysis. The differential signal of the triangle wave is a square wave, and a square wave also appears in the output of the IFOG. The differential signal of

the sine wave has a $\pi/2$ phase difference from the original signal, and the simulation result is again consistent with our analysis.

When $0 < k_f < k_{max}$, we simulate the output signal of the IFOG with the coefficient k_f decreasing gradually, and the simulation results are shown in Figure 2b–d. With the decrease in the coefficient k_f, the crosstalk signal in the gyroscope gradually changes from the differential signal of the LSP to the LSP signal. The simulation results are in line with the expected analysis results.

3. Principle of the Compensation Method

When the LSP fluctuation is not considered, the corresponding light intensity with and without rotation is shown in Figure 3a,c, respectively. The output of the gyroscope can be obtained by integrating the difference between the light intensity of the first and the second half period.
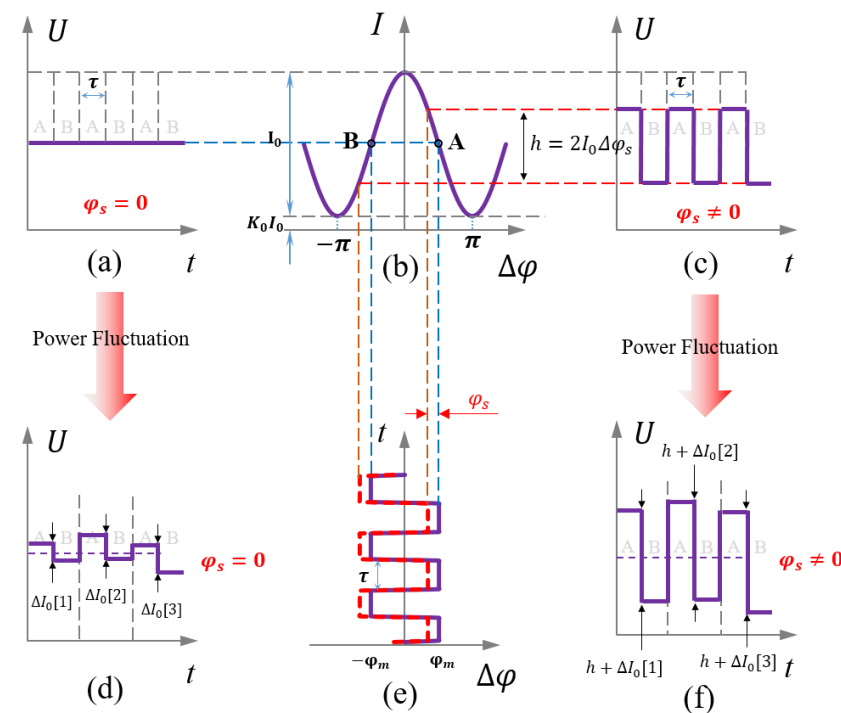
Figure 3. The light intensity of first half period and second half period. (**a**) The light intensity without rotation. (**b**) Response function of light intensity. (**c**) The light intensity with rotation. (**d**) After considering LSP fluctuation, the light intensity without rotation. (**e**) The modulated bias phase. (**f**) After considering LSP fluctuation, the light intensity with rotation.

After considering power fluctuations, the corresponding light intensity with and without rotation is shown in Figure 3d,f, respectively. Due to the LSP fluctuation, even if the rotation does not change, there will be a difference in the light intensity between the first and the second half period. In the first half period $(0\sim\tau)$, the interference light intensity is $I_0(1 - \Delta\varphi_s)$. In the second half period $(\tau\sim2\tau)$, the interference light intensity is $(I_0 + \Delta I_0)(1 + \Delta\varphi_s)$. The difference in the interference light intensity between the first half period and the second half period is $2I_0\Delta\varphi_s + \Delta I_0 + \Delta I_0\Delta\varphi_s$. However, both ΔI_0 and $\Delta\varphi_s$ are very small, so the interference light intensity difference can be expressed as $2I_0\Delta\varphi_s + \Delta I_0$. Therefore, the difference in light intensity, ΔI_0, caused by LSP fluctuation will be also integrated into the output of the gyroscope. Therefore, the key to compensating for the LSP fluctuations is calculating the ΔI_0 in real-time.

We present two methods for the real-time demodulation of ΔI_0, double period modulation (DPM) and triple period modulation (TPM). The two methods have their own advantages. The performance of DPM is better, but it is difficult to realize in a miniature

fiber-optic gyroscope. Therefore, we present the method of TPM, which can be used in micro-optic fiber gyroscopes, but its performance is slightly worse.

3.1. Principle of DPM

In the traditional IFOG, a square wave is generally used to set the bias phase, and we divide the square wave modulation into six stages (A, B, C, D, E, and F), as shown in Figure 4a. In the B and E stages, we modulate the bias phase to $\pm\varphi_m$, but in the A, C, D, and F stages, we modulate the bias phase to zero. When the square wave and step wave are superimposed, the phase of the two beams rotating in opposite directions is shown in Figure 4c.
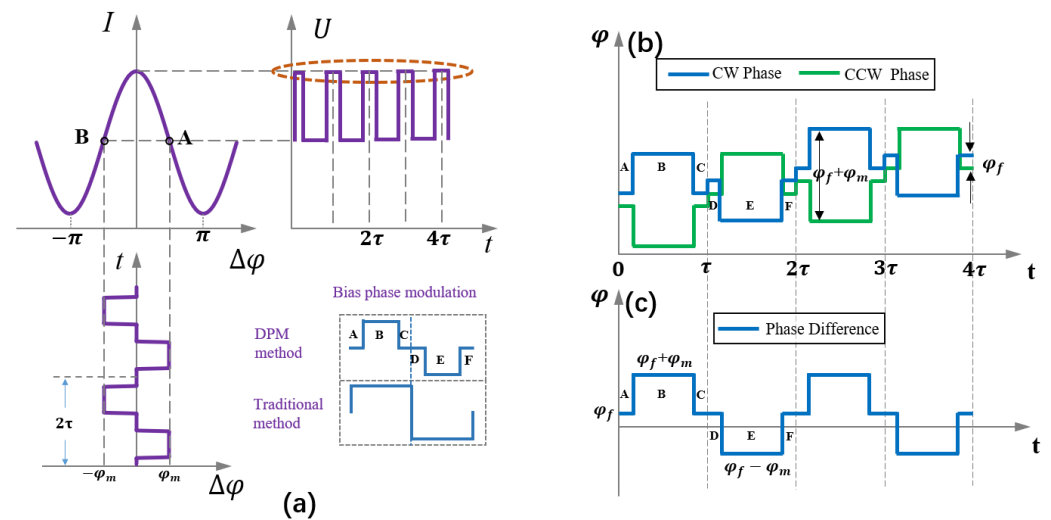
Figure 4. Light source power demodulation method of DPM. (**a**) Improved principle of square-wave bias modulation. (**b**) Modulation phase of CW and CCW light. (**c**) Phase difference between CW and CCW light.

When $\varphi_m = \pi/2$, the phase difference, φ_{smf}, of the two beams rotating in opposite directions can be expressed as follows, at each stage.

$$\varphi_{smf} = \begin{cases} AC: & \Delta\varphi_s \\ DF: & \Delta\varphi_s \\ B: & \Delta\varphi_s + \pi/2 \\ E: & \Delta\varphi_s - \pi/2 \end{cases} \tag{8}$$
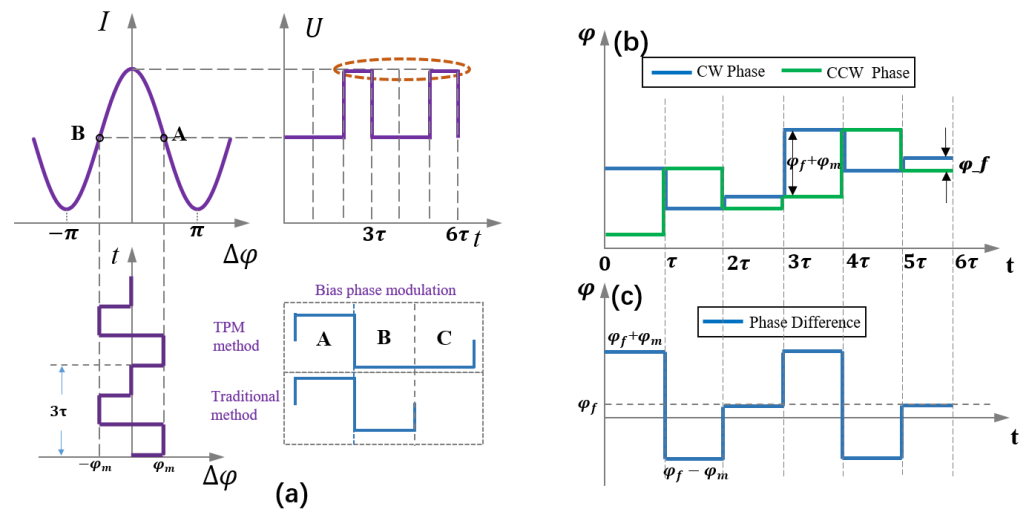
where $\Delta\varphi_s \to 0$. Therefore, the light intensity at each stage can be expressed as follows.

$$I = \begin{cases} AC: & I_0(1+K_0) \\ DF: & I_0(1+K_0) \\ B: & I_0(1+K_0-\Delta\varphi_s) \\ E: & I_0(1+K_0+\Delta\varphi_s) \end{cases} \tag{9}$$

where K_0 is caused by the incomplete cancellation of the two counter-rotating beams [23]. From Equation (8), we know that the phase difference between the two counter-rotating beams in stages A, C, D, and F is close to zero. However, the light intensity response is a cosine function, and the slope is zero at the origin. Therefore, the light intensity in stages A, C, D, and F is linearly related to the power of the light source. Finally, the average light intensity of the D and F stages minus the average light intensity of the A and C stages can reach $\Delta I_0 = I_{DF} - I_{AC}$.

3.2. Principle of TPM

In a miniature fiber-optic gyroscope, the length of the fiber coil is very short, only 100–200 m. The time it takes for the light to pass through the fiber coil is also very short, perhaps less than 1 μs. The DPM method requires the division of a period into several parts, which greatly increases the requirements for the circuit and may significantly affect the performance of the gyroscope [24]. Therefore, we use the method of TPM. The control period of the traditional fiber-optic gyroscope is 2τ, but the control period in TPM is 3τ. We add a period of τ to the traditional square wave modulation, and this period τ modulates the bias phase to zero, as shown in Figure 5a. When the square-wave bias phase and the step-wave feedback phase are superimposed, the modulation phases of clockwise (CW) and counterclockwise (CCW) light are shown in Figure 5b, and the phase difference is shown in Figure 5c.

Figure 5. Light source power demodulation method of TPM. (**a**) Improved principle of square-wave bias modulation. (**b**) Modulation phase of CW and CCW light. (**c**) Phase difference between CW and CCW light.

When $\varphi_m = \pi/2$, the phase difference φ_{smf} of the two beams rotating in opposite directions can be expressed as follows, at each stage.

$$\varphi_{smf} = \begin{cases} A : \Delta\varphi_s + \pi/2 \\ B : \Delta\varphi_s - \pi/2 \\ C : \Delta\varphi_s \end{cases} \tag{10}$$

where $\Delta\varphi_s \to 0$; therefore, the light intensity at each stage can be expressed as follows.

$$I = \begin{cases} A : I_0(1 + K_0 - \Delta\varphi_s) \\ B : I_0(1 + K_0 + \Delta\varphi_s) \\ C : I_0(1 + K_0) \end{cases} \tag{11}$$

From Equation (10), we know that the phase difference between the two counter-rotating beams in the C stage is close to zero. However, the light intensity response is a cosine function, and slope is zero at the origin. Therefore, the light intensity in stage C is linearly related to the power of the light source. By calculating the light intensity difference between adjacent periods, we can obtain $\Delta I_0 = (I_C[n] - I_C[n-1])/3$.

4. Experiment

4.1. Error Verification Experiment

When $k_f \to k_{max}$, we modulate the driving current into a square wave, triangle wave, and sine wave, with a bias of 100 mA, a frequency of 2 kHz, and an amplitude of 1 mA. Figure 6 shows the output signal of the gyroscope and the modulated current signal. When the square wave of the driving current jumps, the gyroscope's output signal displays a peak pulse. The square wave signal is superimposed on the output of the gyroscope when the driving current is a triangle wave. When the driving current is a sine wave, the output signal of the gyroscope displays a sine signal with a phase difference of $\pi/2$ from the drive current signal. All experimental results shown in Figure 6 agree with the simulation results shown in Figure 2a.
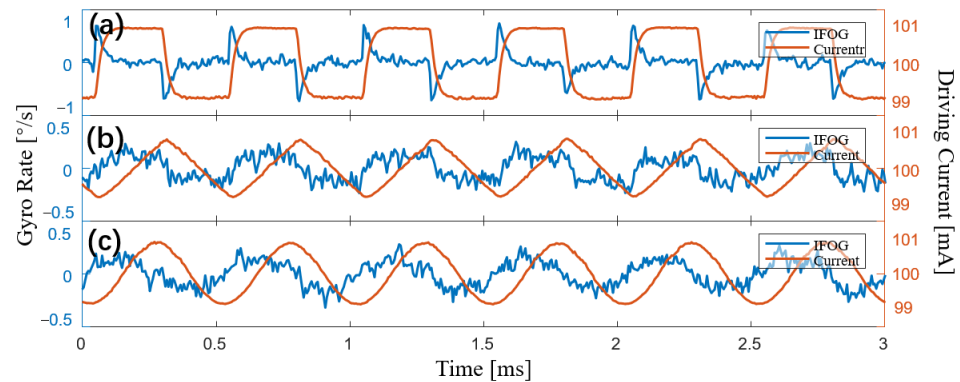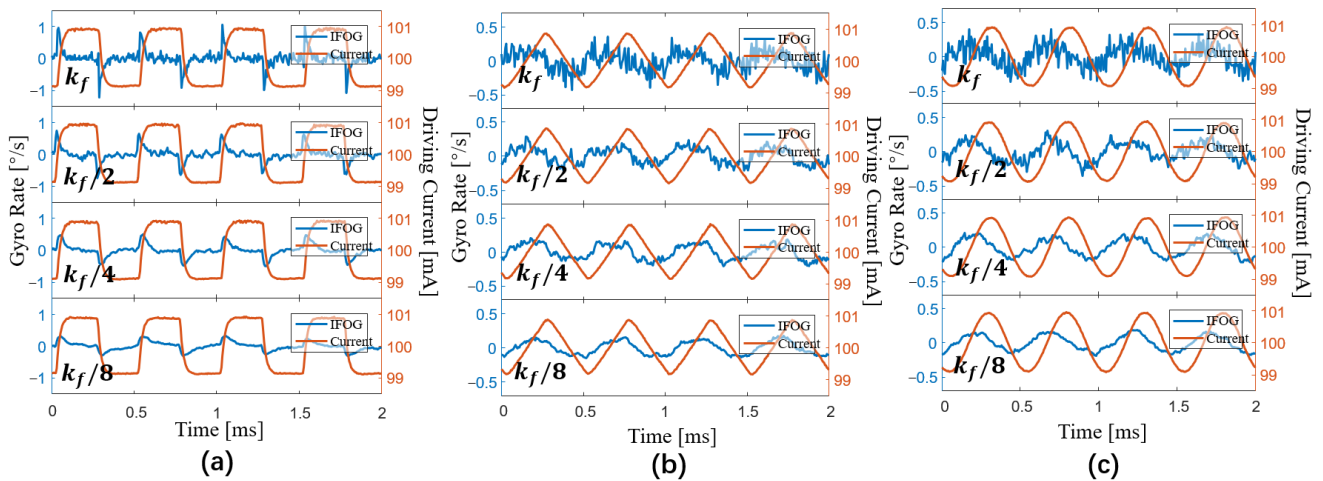

Figure 6. Experimental results of the output signal of the gyroscope and driving current of the light source. (**a**) Measurement results when the driving current is a square wave. (**b**) Measurement results when the driving current is a triangle wave. (**c**) Measurement results when the driving current is a sine wave.

When $0 < k_f < k_{max}$, the crosstalk signal in the gyroscope is no longer the differential signal of LSP. With a bias of 100 mA, a frequency of 2 kHz, and an amplitude of 1 mA, we modulate the driving current into a square wave, a triangle wave, and a sine wave, respectively. As shown in Figure 7, the output signal of the IFOG is measured as the coefficient k_f decreases gradually. When the coefficient k_f gradually decreases, the crosstalk signal in the output signal of the gyroscope eventually transforms from the differential signal of the LSP to the LSP signal itself. The experimental results, given in Figure 7, are consistent with the simulation results, presented in Figure 2b–d.

The two groups of experiments show that when the condition ($k_f \to k_{max}$) is satisfied, the output signal of the gyroscope crosstalk the differential signal of the LSP. By subtracting a certain proportion of the differential signal of the LSP from the gyroscope's output signal, it is able to effectively reduce the impact of LSP fluctuations [22]. However, this condition ($k_f \to k_{max}$) is not satisfied in most practical applications, because the value of the coefficient k_f is different in different applications. Thus, the compensation method of subtracting a certain proportion of the differential signal of the LSP from the gyroscope's output signal fails to achieve the desired results.

We add the feature of compensating for the fluctuations of LSP to the closed-loop control of the traditional gyroscope. For this method, the value of the variable ΔI_0 must be known in real-time, and we can demodulate ΔI_0 using the DPM and TPM methods. The following sections detail the compensation results and the performance difference between DPM and TPM.
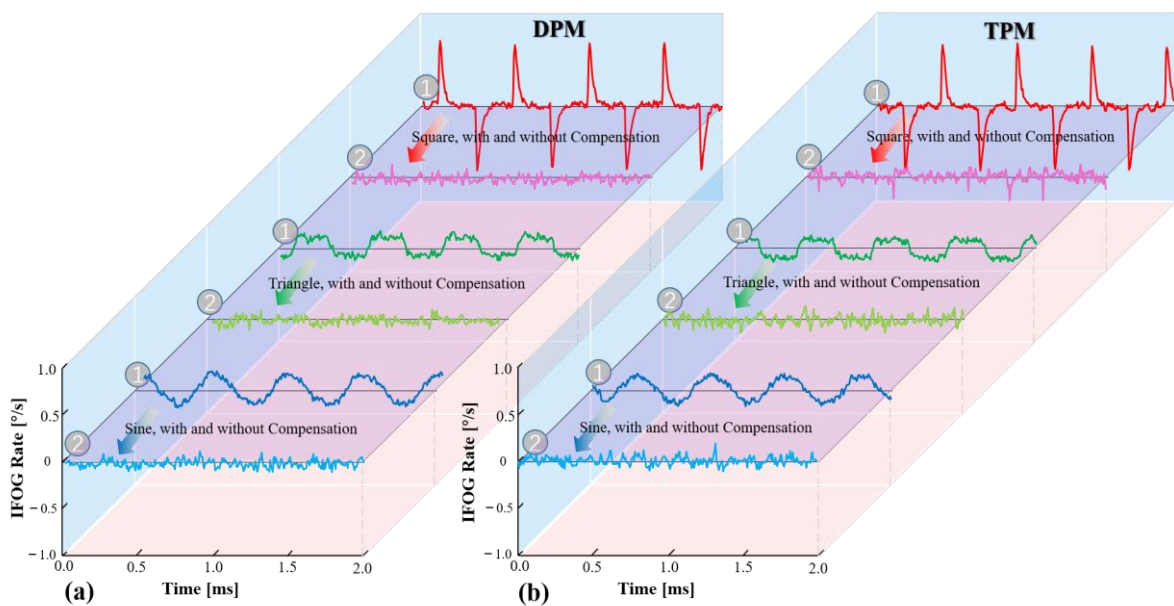
Figure 7. Experimental results of the output signal of the gyroscope when k_f gradually decreases. (**a**) Results of the square-wave driving current. (**b**) Results of the triangle-wave driving current. (**c**) Results of the sine-wave driving current.

4.2. Light Source Power Compensation in Closed-Loop Control

The key to compensating LSP fluctuations is to acquire ΔI_0. We present two methods for obtaining ΔI_0: DPM and TPM. DPM's frequency of demodulating ΔI_0 is three times that of TPM, leading to better performance. Unfortunately, DPM must split a period into three parts, which significantly increases the circuit's requirements. With a micro gyroscope, the length of the fiber coil is relatively short, and hence the period may be less than 1 μs, making it difficult to use the DPM method. As such, we propose the TPM method, which does not raise the circuit's requirements.

With a bias of 100 mA, a frequency of 2 kHz, and an amplitude of 2 mA, we modulate the driving current into a square wave, a triangle wave, and a sine wave in the experiment. The output signal of the gyroscope is then measured with and without compensation, as shown in Figure 8, where the curve labelled "1" represents the output signal without compensation and the curve labelled "2" represents the output signal with compensation.


Figure 8. Experimental measurement results of the output signals of the gyroscope with and without compensation. (**a**) The result of the DPM method. (**b**) The result of the TPM method.

Figure 8 shows that both the DPM and TPM methods are effective and that the mistake produced by the LSP fluctuations has been adequately compensated for. To further evaluate the performance difference between the two compensation methods, we modulated the driving current of the light source using various waveforms and amplitudes, as shown in Table 1. Figure 9 shows the results of measuring the bias stability of the gyroscope with and without DPM and TPM compensation.

Table 1. Parameters of the drive current.

| Waveform	Frequency	Amplitude
Square		0.5 mA
Triangle	2 kHz	1.0 mA
Sine		2.0 mA
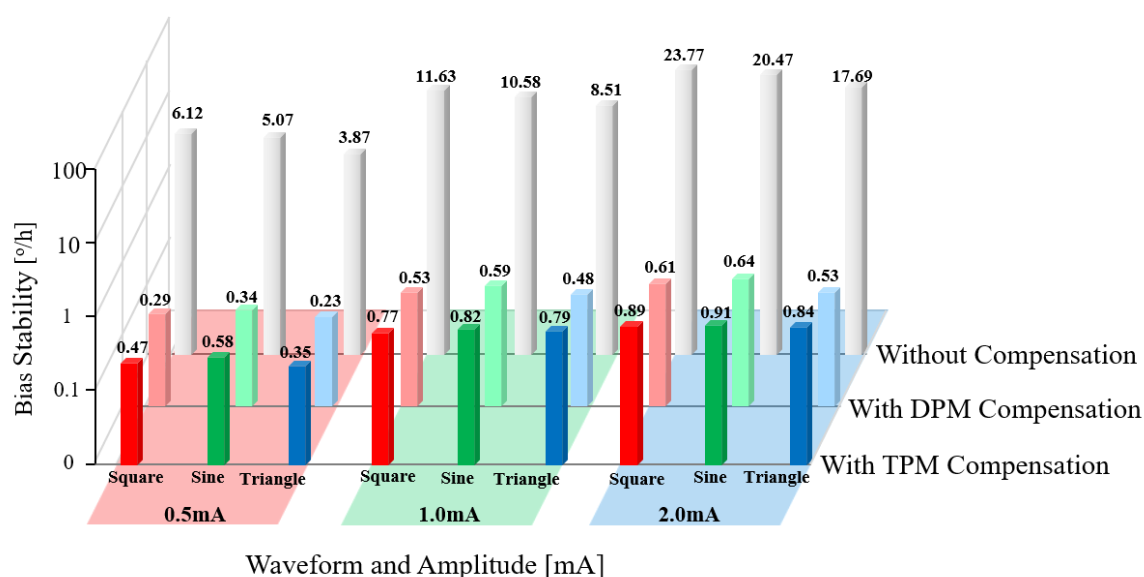
Figure 9. Experimentally measured bias stability of gyroscopes with different driving currents, and the bias stability of a gyroscope with the compensation of DPM and TPM.

When the light source is controlled by a constant temperature and current, the gyroscope's bias stability is 0.089 °/h. The bias stability of the gyroscope degrades by two to three orders of magnitude when the driving current of the light source is intentionally modulated to create power fluctuations, as shown in Figure 9. In addition, for every 0.1 mA increase in the amplitude of the driving current, the bias stability of the gyroscope degrades by 8 to 13 times, compared to the case when the light source is controlled by a constant temperature and current. Both DPM and TPM can efficiently decrease the error caused by the fluctuations in the LSP. As shown in Table 2, we examined the variance in bias stability between DPM and TPM.

Figure 9 and Table 2 show that both DPM and TPM compensation methods increase bias stability by more than 90%. DMP's higher improvement percentage, about 3–5%, is mostly attributable to its higher frequency for ΔI_0 demodulation than that of TPM. When the frequency of LSP fluctuation is relatively low (as shown in Figure 10a,b), the higher the frequency, the greater the difference in light intensity between the first half period and the second half period. However, when the frequency of the LSP fluctuation is too high, the light intensity difference will be very small, as shown in Figure 10c–e. That is to say, power fluctuations in a certain frequency range have the greatest effect on the gyroscope, and this range depends on the length of the fiber coil.

Table 2. Bias stability of gyroscopes with different driving currents.

Waveform	Amplitude	Bias Stability without Compensation (°/h)	Bias Stability with DPM Compensation (°/h)	Bias Stability with TPM Compensation (°/h)
Square	0.5 mA	6.12	0.29 (↓95.3%)	0.47 (↓92.3%)
Square	1.0 mA	11.63	0.53 (↓95.4%)	0.77 (↓93.4%)
Square	2.0 mA	23.77	0.61 (↓97.4%)	0.89 (↓96.3%)
Sine	0.5 mA	5.07	0.34 (↓93.3%)	0.58 (↓88.6%)
Sine	1.0 mA	10.58	0.59 (↓94.4%)	0.82 (↓92.2%)
Sine	2.0 mA	20.47	0.64 (↓96.9%)	0.91 (↓95.6%)
Triangle	0.5 mA	3.87	0.23 (↓94.1%)	0.35 (↓91.0%)
Triangle	1.0 mA	8.51	0.48 (↓94.4%)	0.79 (↓90.7%)
Triangle	2.0 mA	17.69	0.53 (↓97.0%)	0.84 (↓95.3%)
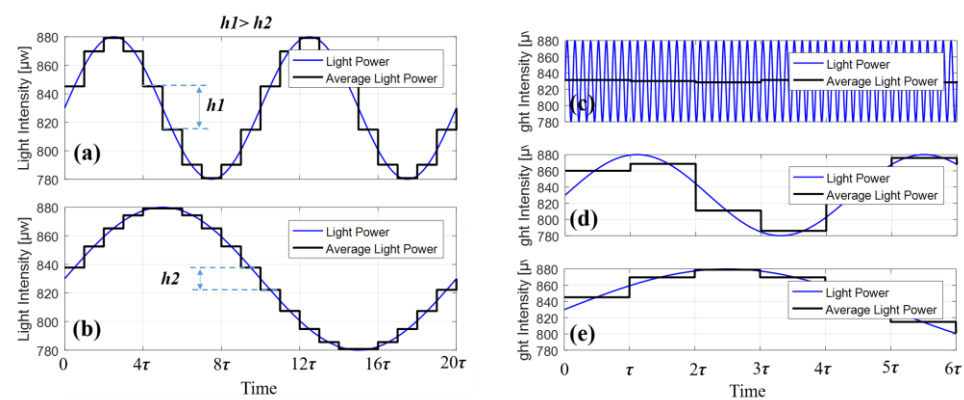
Figure 10. The difference in light intensity under different frequencies. (**a**,**b**) When the frequency is relatively low, the higher the frequency, the greater the error ($h_1 > h_2$). (**c**–**e**) When the frequency is too high and too low, the error becomes very small.

To further test the performance of the two compensation methods at different frequencies of LSP fluctuations, the driving current of the light source is modulated into a sine wave with an amplitude of 1 mA and frequencies of 1 kHz, 2 kHz, 4 kHz, 8 kHz, and 16 kHz. Figure 11 shows the results of a comparison of the bias stability of gyroscopes with DPM and TPM compensation at various frequencies of LSP fluctuations.
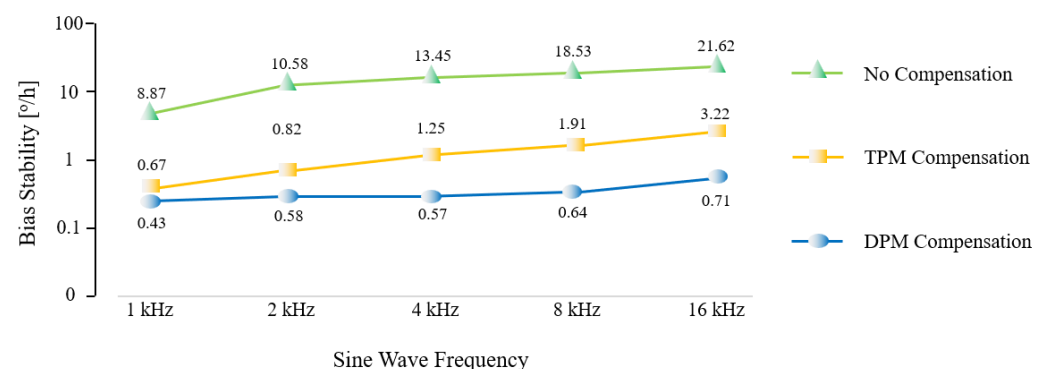
Figure 11. Experimentally measured bias stability of gyroscopes with different frequencies of light source power fluctuations, and the bias stability of gyroscopes with DPM and TPM compensation.

As shown in Figure 11, the bias stability of the gyroscope degrades as the frequency of the LSP fluctuations increases. Both the DPM and TPM methods are able to effectively reduce the detrimental effects of the LSP fluctuations, despite the varying frequency of the LSP fluctuations. When the frequency of the LSP fluctuations gradually rises, the

performance of the DPM remains almost the same, but the performance of the TPM drops slightly; this is mostly due to the higher frequency of the ΔI_0 demodulation of the DPM. The TPM demodulates ΔI_0, based on the light intensity of adjacent periods, with a relatively low demodulation frequency. Thus, there is some performance reduction, but TPM can also achieve a bias stability improvement of over 80%. In actual applications, if the fiber coil is fairly long and there is sufficient time for light to pass through, we can pick the DPM compensation method. Unfortunately, with a small fiber coil, the time necessary for light to pass through the fiber coil is very short, making DPM not feasible. In this case, TPM can be used, since it also achieves an acceptable level of compensation.

5. Conclusions

The power fluctuations of the light source have a direct effect on the IFOG's output signal, which has a significant effect on the IFOG's performance. Nowadays, IFOG's performance is close to its theoretical limit, and the miniaturization and low cost of IFOG have become hot topics of study. Throughout the miniaturization and cost-reduction processes, the light source may be integrated and simplified, which affects its stability and results in power fluctuations. We studied the effect of light source power fluctuations on the IFOG under various coefficients k_f, and found that the effect of LSP fluctuations vary with k_f. We present two methods of compensation, DPM and TPM, both of which can provide adequate compensation for any coefficient k_f. Both DPM and TPM have achieved about 95% increase in bias stability, with DPM performing slightly better than TPM. Regrettably, DPM is difficult to achieve in the application of tiny fiber coils, but TPM can be applied in any gyroscope and has acceptable compensation performance. Our work increases the possibility of employing simpler light sources and driving circuits (e.g., no TEC, no constant temperatures control, and no constant current control) in IFOG, which has significant implications for ongoing attempts to miniaturize and lower the cost of fiber-optic gyroscopes.

Author Contributions: All the authors made contributions to this work. This was originally the idea of S.Z. and G.F.; S.Z. proposed the scheme, developed the algorithms, completed the simulation, and wrote this manuscript; M.R., X.L. and H.Z. performed the experiments; and G.F. supervised all the work and improved this manuscript. All authors have read and agreed to the published version of the manuscript.

Institutional Review Board Statement: Not applicable.

Informed Consent Statement: Not applicable.

Data Availability Statement: The data used to support the findings of this study are available from the corresponding author upon reasonable request.

Conflicts of Interest: The authors declare no conflict of interest.

References

1. Sanders, G.A.; Sanders, S.J.; Strandjord, L.K.; Qiu, T.; Wu, J.; Smiciklas, M.; Mead, D.; Mosor, S.; Arrizon, A.; Ho, W. Fiber optic gyro development at Honeywell. In Proceedings of the Fiber Optic Sensors and Applications XIII, Baltimore, MD, USA, 12 May 2016; p. 985207.
2. Pavlath, G. Recent improvements in fiber optic gyros at Northrop Grumman Corporation. *Opt. Waveguide Laser Sens.* **2020**, *11405*, 1140506.
3. Shang, K.; Lei, M.; Xiang, Q.; Na, Y.; Zhang, L.; Yu, H. Near-navigation-grade interferometric fiber optic gyroscope with an integrated optical chip. *Chin. Opt. Lett.* **2020**, *18*, 120601. [CrossRef]
4. Shang, K.; Lei, M.; Xiang, Q.; Na, Y.; Zhang, L. Tactical-grade interferometric fiber optic gyroscope based on an integrated optical chip. *Opt. Commun.* **2021**, *485*, 126729. [CrossRef]
5. Qi, Y.; Feng, W.; Li, F.; Hu, T.; Wang, Y.; Wang, N. An ultra-short coil fiber optic gyroscope. *Opt. Laser Technol.* **2023**, *157*, 108751. [CrossRef]

6. Suo, X.; Yu, H.; Wu, X. Integrated Interferometric Fiber Optic Gyroscope Employing a Photo-Electronic Chip. *IEEE Photonics Technol. Lett.* **2022**, *34*, 1250–1253. [CrossRef]
7. Gundavarapu, S.; Belt, M.; Huffman, T.A.; Tran, M.A.; Komljenovic, T.; Bowers, J.E.; Blumenthal, D.J. Interferometric Optical Gyroscope Based on an Integrated Si3N4 Low-Loss Waveguide Coil. *J. Light. Technol.* **2018**, *36*, 1185–1191. [CrossRef]
8. Bischel, W.; Kouchnir, M.; Bitter, M.; Yahalom, R.; Taylor, E. Hybrid integration of fiber optic gyroscopes operating in harsh environments. *Nanophotonics Macrophotonics Space Environ. V* **2011**, *8164*, 197–204.
9. Rickman, A. The commercialization of silicon photonics. *Nat. Photonics* **2014**, *8*, 579–582. [CrossRef]
10. Tran, M.A.; Komljenovic, T.; Hulme, J.C.; Kennedy, M.J.; Blumenthal, D.J.; Bowers, J.E. Integrated optical driver for interferometric optical gyroscopes. *Opt. Express* **2017**, *25*, 3826–3840. [CrossRef] [PubMed]
11. Wang, L.; Halstead, D.R.; Monte, T.D.; Khan, J.A.; Brunner, J.; Heyningen, M.A.K.v. Low-cost, High-end Tactical-grade Fiber Optic Gyroscope Based on Photonic Integrated Circuit. In Proceedings of the 2019 IEEE International Symposium on Inertial Sensors and Systems (INERTIAL), Naples, FL, USA, 1–5 April 2019; pp. 1–2.
12. Shang, K.; Lei, M.; Li, H.; Zhang, T.; Yu, X.; Xiang, Q.; Na, Y.; Zhang, L. Ultra-small interferometric fiber optic gyroscope with an integrated optical chip. *Chin. Opt. Lett.* **2022**, *20*, 040601. [CrossRef]
13. Hui, F.; Tianjin, M.L.; Ma, L.; Zuo, W.; Zhang, S.; Zhang, X.M. Investigation on near Gaussian-shaped spectrum erbium-doped fiber source which applied to the fiber optic gyroscope. In Proceedings of the 2017 24th Saint Petersburg International Conference on Integrated Navigation Systems (ICINS), Saint Petersburg, Russia, 29–31 May 2017; pp. 1–4.
14. Fei, H.; Mao-chun, L.; Lin, M. Double-Pass Backward ASE light source which applied to the three-axis FOG. *J. Chin. Inert. Technol.* **2016**, *24*, 158–162.
15. Chen, X.; Yang, J.; Zhou, Y.; Shu, X. An improved temperature compensation circuit for SLD light source of fiber-optic gyroscope. *J. Phys. Conf. Ser.* **2017**, *916*, 012027. [CrossRef]
16. Çelikel, O.; San, S.E. Design details and characterization of all digital closed-loop interferometric fiber optic gyroscope with superluminescent light emitting diode. *Opt. Rev.* **2009**, *16*, 35–43. [CrossRef]
17. Zhang, C.; Zhang, S.; Pan, X.; Jin, J. Six-state phase modulation for reduced crosstalk in a fiber optic gyroscope. *Opt. Express* **2018**, *26*, 10535–10549. [CrossRef] [PubMed]
18. Vali, V.; Shorthill, R.W. Fiber ring interferometer. *Appl. Opt.* **1976**, *15*, 1099–1100. [CrossRef] [PubMed]
19. Xue, L.; Zhou, Y.; Li, J.; Liu, W.; Xing, E.; Chen, J.; Tang, J.; Liu, J. Error analysis of dual-polarization fiber optic gyroscope under the magnetic field-variable temperature field. *Opt. Fiber Technol.* **2022**, *71*, 102926. [CrossRef]
20. Cao, Y.; Xu, W.; Lin, B.; Zhu, Y.; Meng, F.; Zhao, X.; Ding, J.; Lian, Z.; Xu, Z.; Yu, Q.; et al. A method for temperature error compensation in fiber-optic gyroscope based on machine learning. *Optik* **2022**, *256*, 168765. [CrossRef]
21. Li, J.; Zhou, Y.; Xue, L.; Liu, W.; Xing, E.; Tang, J.; Liu, J. Magnetic error suppression in Polarization-Maintaining fiber optic gyro system with orthogonal polarization states. *Opt. Fiber Technol.* **2022**, *71*, 102927. [CrossRef]
22. Zheng, S.; Ren, M.; Luo, X.; Zhang, H.; Feng, G. Real-Time Compensation for SLD Light-Power Fluctuation in an Interferometric Fiber-Optic Gyroscope. *Sensors* **2023**, *23*, 1925. [CrossRef] [PubMed]
23. Li, X.; Zhang, Y.; Zhang, C. Five Points Modulation in Closed Loop Fiber Optic Gyroscope. In Proceedings of the 2009 5th International Conference on Wireless Communications, Networking and Mobile Computing, Beijing, China, 24–26 September 2009; pp. 1–3.
24. Qi, Y.; Zhang, X.; Wang, Y.; Wang, M.; Liu, Z.; Gong, C.; Liu, Y. Application of a novel spatial non-reciprocal phase modulator in fiber optic gyroscope. *Opt. Fiber Technol.* **2020**, *58*, 102258. [CrossRef]